Single and Multiple Scattering Components of the Surface Current for Rough Surface Scattering

Ernesto Rodríguez
Jet Propulsion Laboratory
California Institute of Technology
4800 Oak Grove Dr., Pasadena, CA 91109

(Submitted to JOSA)

For enquiries, contact ed@dionysus.jpl.nasa.gov

Abstract

A method is presented for separating the single and multiple scattering contributions to the surface current which is valid up to second order in perturbation theory. Using this method, numerical experiments are performed to determine the spectral characteristics of the surface current as a function of incidence angle and surface roughness for long random periodic gratings. It is shown that as the incidence angle increases, the single scattering contribution shows a dependence on surface slope which is not present in standard perturbation theories. The higher order surface current and scattered field are also calculated and shown to be consistent with a double-bounce scattering mechanism for most incidence angles. However, it is shown that very close to grazing incidence, the higher order fields are more consistent with an odd number of bounces.

1. Introduction

During the last decade, a number of new approximate solutions to the problem of scattering from rough surfaces have appeared. Two basic types of approach have been suggested: the first type uses a perturbation expansion for the surface current or the transition matrix to derive a perturbation expansion in which the nth power of the surface height spectrum appears as in the nth order term [1], [2], [3], [4], [5], [6], [7], [8]. Alternately, a series may be obtained by iterating the magnetic field integral equation [9], [10], [11]. The two series are not identical, but there are relationships that can be drawn between them in a suitable limit [9]. Although many of these theories give good agreement for specific cases, it is not clear what is the regime of validity for this type of perturbation expansions or their convergence characteristics.

The purpose of this paper is to investigate numerically the validity of the first type of perturbation series. Past numerical comparisons in the literature [12], [13], [14], [15], [16], [17], [18], [19] have concentrated on the comparison of the scattered field at infinity with numerical results. This has the advantage that the accuracy of particular theories can be evaluated in a straightforward fashion. It has the disadvantage, however, that not much insight is gained about the scattering mechanisms which operate on the random surface, or the reasons why any specific theory breaks down beyond its regime of validity. In this paper,

I will examine the surface current, rather than the scattered field, and show how general conclusions about the scattering mechanisms operating on the surface can be drawn.

The usual interpretation of the type of perturbation expansion examined here is that the nth order term represents a scattering interaction during which n Bragg bounces of the incident field occur. In the first section, I show how, given the numerical soultion for the surface current, the first order (single-bounce) contribution can be estimated. Most of the numerical studies mentioned above must compare the analytic predictions for the scattered cross-section for an infinite surface with numerical results for a finite surface. In order to compensate for edge effects, some kind of incident field tapering is introduced [12], [13]. Unfortunately, this tapering introduces distortions in the surface current magnitude and phase which make the analysis of the scattering mechanisms more difficult. In order to overcome this limitation, we examine in this paper long periodic surfaces for which perturbation expansions may also be obtained. Since the emphasis of this paper is in examining scattering mechanisms, rather than computing infinite surface scattering cross-sections, this assumption is not a limiting factor as long as the surface periodicity is large enough that very long range scattering interactions are adequately represented. In the second section and the Appendix, I show how the surface current and scattered field may be computed for one-dimensional periodic rough surfaces with high accuracy even for very high angles of incidence. The third section examines the characteristics of the first-order interaction as a function of surface height and slope, and the incidence angle. Having separated the first-order interaction, it is possible to examine the residual interactions. The next section examines the contribution to multiple scattering as a function of sulfate roughness and incidence angle. Finally, the last section examines the polarimetric characteristics of the scattered field and the validity of interpreting the perturbation expansion as an expansion on the number of interactions with the surface spectrum.

2. Method for Separating the Surface Current

For perfectly conducting surfaces, the surface current, $\vec{J}(r_s)$ is given by the solution of

the integral equation

$$0 = \vec{E}_0(\vec{r}) + i\frac{\eta_0}{k_0}\nabla \times \left(\nabla \times \int dS\; G_0(\vec{r} - \vec{r}_s)\vec{J}(\vec{r}_s)\right) \tag{1}$$

where $\vec{E}_0(\vec{r})$ is the incident field, $G_0(\vec{r} - \vec{r}_s)$ is the free space Green's function; $\vec{r}_s \equiv \vec{\rho} + \hat{z}z$ is a vector to the surface, $\xi(\vec{\rho})$; $\vec{r}$ is the observation point, which is assumed to lie below the surface (i.e., for $z \leq \xi(\vec{\rho})$); k_0 is the wavenumber in free space; and η_0 is the impedance of free space. This equation is called the "Extinction Theorem" [21] because it shows that the incident field below the surface is extinguished by the scattered field.

Rather than analize the surface current directly, I remove the phase variations due to the incident field on the surface, and examine a related quantity, which I call the source function and define it as

$$\vec{F}(\vec{\rho}) = \frac{\eta_0}{2}\left[1 + (\nabla\xi)^2\right]^{1/2}\exp\left[-i\left(\vec{\kappa}_0\cdot\vec{\rho} - p_0\xi\right)\right]\vec{J}(\vec{\rho}) \tag{2}$$

where κ_0 and $-p_0$ are the horizontal and vertical components of the incident wavevector, respectively. It has been argued [22], [6] that the removal of these phase factors, which are required by translational invariance of the surface spectrum, yields a quantity which can be understood more easily in terms of a multiple scattering series.

The Fourier transform of the source function, given by

$$\hat{F}(\vec{\gamma}) = \int d^2\rho\;\exp\left[-i\vec{\gamma}\cdot\vec{\rho}\right]\vec{F}(\vec{\rho}) \tag{3}$$

can be used as a starting point for a perturbation expansion in terms of the surface spectrum

$$\hat{F}(\gamma) \approx \vec{a}_0 + \vec{a}_1(\gamma)\hat{\xi}(\gamma) + \int d^2\gamma'\;\vec{a}_2(\vec{\gamma},\vec{\gamma}')\hat{\xi}(\vec{\gamma} - \vec{\gamma}')\hat{\xi}(\vec{\gamma}') + \ldots \tag{4}$$

where $\hat{\xi}$ is the Fourier transform of ξ. In the previous perturbation expansion, the nth order term contains n factors of the surface Fourier coefficient, and $n-1$ integrals over the intermediate wavenumbers. The nth term is interpreted as the sum of all order n momentum transfers. For each momentum transfer, the scattered wave interacts resonantly with n surface spectral components in such a way that the net transfered momentum corresponds to the change in horizontal momentum of the nth multiply scattered wave relative to the

incident field horizontal momentum. The three terms shown explicitly in the previous equation correspond to the coherent component (no momentum transfer), single scattering (one momentum transfer), and double scattering (two momentum transfers). The expansion coefficients, $\vec{a}(\vec{\gamma}_1, \ldots, \vec{\gamma}_n)$ are the coupling coefficients which one must estimate. Expansions of this type have been used explicitly or implicitly by many perturbation expansion schemes in the literature [1], [2], [3], [4], [5], [6], [7], [8]

Given N realizations of the source function for independent identically distributed random rough surfaces, it is possible to obtain an estimate of the first order coupling coefficient. Assuming that we are dealing with zero-mean Gaussian random surfaces, one has that all odd order moments of the surface spectrum vanish, and the even orders can be expressed in terms of the second order moment

$$\langle \tilde{\xi}(\vec{\gamma}) \tilde{\xi}^*(\vec{\gamma}') \rangle = \delta(\vec{\gamma} - \vec{\gamma}') W(\gamma) \tag{5}$$

where $W(\gamma)$ represents the surface height spectrum for wavenumber $\vec{\gamma}$. Using this fact, one can show that the least squares estimate for the single scattering coupling coefficient, correct up to second order in the perturbation is given by

$$\hat{\vec{a}}_1 = \frac{\sum_{i=1}^{N} \tilde{I}_1^i(\vec{\gamma}) \tilde{\xi}_i^*(\vec{\gamma})}{\sum_{i=1}^{N} \tilde{\xi}_i(\vec{\gamma}) \tilde{\xi}_i^*(\vec{\gamma})} \tag{6}$$

In the limit of infinite number of realizations, this expression converges to $\langle \tilde{F}(\vec{\gamma}) \tilde{\xi}^*(\vec{\gamma}) \rangle / W(\vec{\gamma})$. Since the odd moments of ξ vanish, the even order scattering contributions will act as zero-mean noise terms in the estimation. The odd order contributions, on the other hand, may result non-zero mean contributions, which will bias the estimation. It is not expected that, for the types of surfaces I will deal with in this paper, third and higher order scattering contributions play a significant role, but their contribution is a limiting factor for the method presented here.

To provide a point of comparison, the first order coupling coefficient obtained in the Unified Perturbation Method [6] (UPM), is given by

$$\vec{a}_0 = (2\pi)^2 \delta(\vec{\gamma}) \frac{p_0}{k_0} \left(\hat{e}_0 - k_0 \frac{\hat{e}_0 \cdot \hat{z}}{\hat{k}_0 \cdot \hat{z}} \right) \equiv (2\pi)^2 \delta(\vec{\gamma}) \tilde{F}^{(0)} \tag{7}$$

$$\vec{a}_1(\vec{\gamma}) = -i(p(\vec{\gamma}) - p_0)\hat{F}_0 + \frac{\vec{k}^{(-)}(\vec{\gamma})}{p(\vec{\gamma})}\hat{F}_0 \cdot \vec{\gamma} \tag{8}$$

In these equations, $-p_0$ is the component of the incident wavenumber in the z direction; k_0 is the magnitude of the incident wavenumber; $p(\vec{\gamma})$ is defined by

$$p(\vec{\gamma}) \equiv (k_0^2 - (\gamma_0 + \gamma)^2)^{1/2} \quad \text{Im } p \geq 0 \tag{9}$$

and $\vec{k}^{(-)}(\vec{\gamma})$ by

$$\vec{k}^{(-)}(\vec{\gamma}) = (\gamma_0 - \vec{\gamma}) - \hat{z}p(\vec{\gamma}) \tag{10}$$

The first term in equation (8) has nulls for the wavenumbers coupling to the forward and backscatter directions. The second term contains a pole when $p(\vec{\gamma}) = 0$, i.e., for coupling to surface waves. For the one-dimensional surfaces treated in this paper, the second term vanishes for H(orizontal)-polarized (s-polarized) incident fields, but not for V(ertical)-polarized (p-polarized) fields. This represents the fact that there can be no surface waves for horizontal polarized incident fields and this type of surfaces.

3. Numerical Implementation

Surface current realizations were computed by generating ensembles of Gaussian rough surfaces and using the method of moments (MOM) [23] to solve for each realization of the surface current. The Fourier transform of the source function for each surface was then computed using equations (2) and (3). To estimate the first order coupling function, I subtracted the coherent component of the source function by removing the average over all realizations of the source function. Finally, an estimate for $\vec{a}_1$ was obtained by applying equation (6) to the result.

The random surfaces were generated by making an uncorrelated, unit variance, Gaussian random noise sequence in the wavenumber domain, applying the appropriate filter function, and Fourier transforming to the coordinate domain (for details, see [15]). The surface spectrum was proportional to γ^{-s}, and I examined spectral decays of $s = 3$. This spectral decay is observed in ocean surfaces. I also examined a spectral decay of $s = 2.5$ but do not

Snow the results here since the conclusions drawn from them are similar to the $s = 3$ case. The reason for using a power-law spectrum, aside from possible applications to naturally occurring surfaces, is to allow the interaction of the incident wave momentum with all surface wavevectors, aiding in the retrieval of the first order expansion coefficient for all wavenumbers.

The smallest wavelength present in test surfaces was 0.2λ, where λ is the electromagnetic wavelength. The longest wavelength, Λ, was varied to examine the effects of changing the Correlation length (or the surface slope to height ratio). I examined the longest wavelengths of 102.4A, $51.2\lambda, 25.6\lambda$ Three surface root mean squared (rms) heights were examined: 1λ, 0.5λ, and $0.1\ \lambda$. Figure 1 presents the surface slopes and curvatures for the $s = 3$ surfaces, as well as the fraction of the surface which is in monostatic shadowing. Varying the low-frequency cut-off while keeping the rms height constant allows the isolation of surface slope effects from those due to height and incidence angle.

The biggest problem encountered in MOM calculations from random rough surfaces is the avoidance of edge effects. This problem was recognized long ago by Axline and Fung [12] and various methods have been proposed to deal with it. Currently, the most popular method in the literature is the tapered wave method introduced by Thorsos [13], where the incident field is taken to be a tapered field which satisfies Maxwell's equations approximately, but attenuates the return from the edges so they are neglegible. While this method is very attractive from the numerical standpoint, it is limited by the validity of the tapering approximation. More importantly for our application, due to the multiplication of the surface current by a tapering function, the source function spectrum is distorted in both phase and amplitude.

An alternate way of avoiding edge effects is to assume that the surface is periodic and that the period is large enough so that the scattered field, which now has a discrete angular spectrum, approximates the continuous spectrum from an infinite surface. This will be true if the angular separation between modes is smaller than the angular resolution required to observe the surface. This method was proposed by in [151 and [16] to deal with moderate

incidence angles and the reader is referred there for our conventions. Although the far-field results for the periodic surfaces are not equal to the infinite surface limit results, it is not expected that the physics of the multiple scattering interactions will be significantly affected since one expects most multiple scattering interactions to be due to nearby surface features.

The key to implementing this method is the evaluation of the periodic Green's function and its normal derivative on the surface. In the work cited above, we approximated the Green's function by summing only a few terms of its infinite series representation. While this is adequate for moderate incidence angles it is not sufficient as the incidence angle approaches grazing. Here, I make use of an integral representation of the periodic Green's function obtained by Veisoglu et al. [24] together with some approximations which make the Monte Carlo evaluation computationally efficient. The details of the numerical method are presented in Appendix A.

I used the expressions for the Green's function obtained in Appendix A together with the MOM. For each case studied, I used a total of 100 Monte Carlo realizations and all the calculations were performed using double precision arithmetic. The energy conservation was calculated for each case and was found to be better than 0.1% in all cases, and better than 0.01% in most cases. I estimate that the error bars in our far field scattering results due to speckle are of the order of ±1 dB.

4. First Order Coefficient Results

First order perturbation theory is known to provide adequate predictions for the scattered field for moderate incidence angles (for detailed numerical comparisons, see [15] and [16]). Figure 2 shows the magnitude and phase for the estimated Horizontal and Vertical polarized first-order coefficients, $\tilde{a}_1$, as a function of the normalized wavenumber, γ/k_0, for an incidence angle of 45°, an rms surface roughness of λ, and various values of rms surface slope. It is clear from this figure that the first order perturbation coefficient is independent of surface slope, for this incidence angle and surface rms height. Similar results are obtained when the surface rms height is 0.1 λ and 0.5λ. The figures also agree with the qualitative features predicted by first order perturbation theory. The H-polarization source

function exhibits nulls when $p(\gamma)$ p_0 t he V-polar ization source function, on the other hand, shows a strong peak for - , / k_0 t 1 $\sin\theta_0$), corresponding to the surface w a v e coupling wavenumber. This figure also show . that the noise in t he est imated first-order coefficient is quite small, indicating that first-order scattering dominates for this situation. There is slightly more noise for V-polar ization compared to H-polar ization, suggesting that t he higher order contributions might be larger for this polarization.

For the sake of comparison, Figure 2 also sh IV; s the predictions for t he UI'M perturbation t heory [6]. The agreement between the estimated coefficient and t he UI 'M prediction is very good for H-p olarization for all wavenumbers. I 'or V-polarization, on the other hand, there are significant disagreements for lar ger waver n mbers. Recalling t hat propagating modes exist for -- (1 -t- $\sin\theta_0$) $\leq \gamma/k_0 \leq$ (1 $\sin\theta_0$), one secs that the agreement is excellent for the propagating modes. For the non-propagating modes, which contribute to the near-field, there is significant disagreement in bot h magn it ude and phase. The estimated first order coefficient predicts that significantly g r eater energy will be allocated to for ward propagating evanescent waves, while significantly lower energy will be allocated to back-propagating evanescent waves, with a weak minimum appr ar ing at $\gamma/k_0 \approx$ 3.7. The behaviour of the V-polarized phase also shows significant dev iat ions in both for war d and backpropagating directions, with only small deviat ions in for t he propagating modes. Previous results [] 5], [16] for the far-field have shown good agr eement between pert urbat ion and MOM results, indicating that the deviations in the non-propagating modes plays a significant effect only for the near field. Nevertheless, it was noticed t hat the V-polar ized predictions were slightly inferior to their H-polarized count er part s. 'J 1 ese r emar ks are also valid for smaller rms surface heights, although the phase deviations are simpler: there is a simple sign change at the same location of the approximate null.

We next explore the behaviom of the f ir st or der coefficient. as a function of incidence angle. Figure 3 presents the estimated r esults for an incidence ang le of 89° and O. 1λ surface rms height. These results are consistent with t he 45° results, However, one now begins to notice a slight dependence of the first or der coefficient on the rms slope for V-polarization.

This dependence increases as the surface rms height increases, as Figure 4 shows for an rms height of λ. This figure shows that, for H-polarization, there is no noticeable slope dependence in either phase or amplitude and the agreement with the UPM prediction is excellent. For V-polarization, on the other hand, there is a very strong dependence of the first-order coefficient on the surface rms slope, with the magnitude of the coefficient decreasing monotonically with slope. The deviations are also seen to be smaller for the propagating modes than for the non-propagating modes. The dependence of the V-polarized magnitude on rms surface slope also increases monotonically with incidence angle. Figure 5 shows the magnitude of the V-polarized first order coefficient for incidence angles Of 60°, 70°, 80", and 85°. Aside from the increased dependence on the slope, this figure also shows that the region in momentum space where back-propagating waves are fOI bidden gets more sharply localized as the! incidence angle increases. 1 currently have no explanation for the existence of this forbidden region.

What causes perturbation theory to agree well with H-polarization, while giving increasingly erroneous results for V-polarization? I have no definite answer to this question, but one notices that for one-dimensional surfaces the solution of the H-polarization perturbation series is correct to all orders of the surface slope. For V-polarization, on the other hand, one must expand the perturbation series in powers of both height and surface slope. Slope corrections contribute to higher order terms, causing a mixing of single and multiple scattering in the perturbation series. For full two-dimensional surfaces, it is necessary to expand in both heights and slopes for both polarizations and one expects H-polarization to show a similar slope dependence in this case. One concludes that the validity of the perturbation series in equation (4), and its interpretation as a multiple scattering series, is limited to the small slope approximation, in agreement with the work of Voronovich [8]. A more accurate series expansion must include slope dependence even in the first-order expansion term.

5. Source Function Results

Having obtained the first-order expansion term, it is now possible to separate the source

function into (approximate) single and multiple scattering terms, and to study the dependence of higher order terms on incidence angle and surface rms height. Figure 6 shows a comparison of the magnitude of the first and higher order components of the source function for both incident polarizations, an incidence angle of 60°, an rms surface height of λ and two values of the surface slope. In comparing the two components, we see that both first and higher order components of the source function have similar characteristics. Both show strong peaks around the coherent direction ($\gamma = 0$). The higher order H-polarized source function shows nulls in the same places as the first order source function, while the V-polarized source function also shows a peak for coupling to back-propagating surface waves.

For the smoother surface, the higher order source function is approximately one order of magnitude smaller than the first order source function in the regions away from the coherent and surface coupling peaks. In the peak regions, however the higher order source function is larger than the first order source function. The rougher surface, on the other hand, has smaller magnitudes for the propagating waves, but slightly higher magnitudes for the non-propagating waves. The shapes of the peaks have become wider and the energy is much more uniformly distributed throughout the spectrum.

We next examine the higher order source function for near-grazing (89°) incidence angles (Figure 7). Unlike the 60° incidence angle case, the magnitude of the higher order source function is comparable to, or higher than, the first-order source function. Furthermore, the shape of both the higher-order source function resembles the shape of the first-order source function. The main difference is that both peaks and nulls have been smoothed out in the higher order source function, These results indicate that higher order scattering becomes of similar importance to single scattering as the angle of incidence increases, and this result will be borne out by the far-field results of the next section. This result gives an indication that the smallness parameter in the scattering expansion is not $p_0\xi$, which approaches zero as the incidence angle approaches grazing, as is sometimes stated in the literature. According to that picture, first order scattering should improve as an approximation as the incidence

angle increases. The importance of multiple scattering, however, should be clear due to the fact that shadowing is intrinsically a multiple scattering phenomenon.

To further study the nature of the interaction between the various Fourier components of the surface, one computes the source function spectrum in Figure 8 for a surface whose Fourier components of wavelength smaller than λ have been removed for an incidence angle of 89°, an rms height of λ, and two values for the rms surface slope. For all the surfaces, the spectrum of the source function shows a dramatic fall-off for wavelengths smaller than the Bragg cutoff while remaining unchanged for the larger wavelengths. The suddenness of the fall-off is greater for H-polarization and for the smoother surfaces. These results indicate that, even though I have established that multiple scattering plays an important role for this incidence angle, the higher order coupling coefficients are still localized in Fourier space; i.e., multiple scattering momentum transfers occur only between waves which are near in Fourier space. Mechanisms of energy transfer which are localized in real space, such as shadowing, do not seem to play a major role in determining momentum transfers for wavelengths comparable to the electromagnetic wavelength. This is physically plausible since one expects that smaller scatterers will cause diffraction rather than shadowing.

As an interesting feature, notice that the enhancement at p(7) = 0 is still present for vertical polarization, even though the resonant waves have been removed. This is in qualitative agreement, with the higher order predictions of UPM [6]. Notice also that once the single scattering component is removed, enhancements of the surface spectrum for wavelengths equal to $\lambda/4$ appear. These enhancements are present for both horizontal and vertical polarizations and for the three surface types. I do not have an explanation for the behavior at this time.

6. Far Field Results

In this section, I examine the contributions of the first and higher order source functions to the scattered field at infinity. For one dimensional surfaces, the complete polarimetric Stokes matrix has only four non-zero elements [25]. Rather than using the Stokes matrix elements, in this paper I will examine the following parameters which contain the same

information but are easier to interpret physically:

$$\sigma_0^{(V)}(\theta_n) \quad k\,1\,\cos^2\theta_i < E_V(\theta_n)E_V^*(\theta_n) > \tag{11}$$

$$\sigma_0^{(H)}(\theta_n) \quad k\,L\cos^2\theta_i < E_H(\theta_n)E_H^*(\theta_n) > \tag{12}$$

$$\gamma(\theta_n) \quad \frac{|< E_V(\theta_n)E_H^*(\theta_n) >|}{\sqrt{< |E_H(\theta_n)|^2 >< |E_V(\theta_n)|^2 >}} \tag{13}$$

$$\Phi(\theta_n) \quad \mathrm{Arg}(< E_V(\theta_n)E_H^*(\theta_n) >) \tag{14}$$

where θ_n is the scattering angle for the nth propagating mode and is given by the grating equation

$$\sin\theta_n = \sin\theta_0 + \frac{n}{L/\lambda} \tag{15}$$

$E_H(\theta_n)$ and $E_V(\theta_n)$ are, respectively, the horizontal and vertically polarized scattering modes, and I have normalized the bistatic cross section such that it agrees with nonperiodic surface case after integrating over all scattering angles [19]. The parameters γ and Φ represent the magnitude of the field correlation and the relative phase difference between the H- and V-polarized fields. In the Small Perturbation Method (SPM) or Physical Optics limits the correlation should be unity and the H and V fields should be out of phase by 180°. Deviations from these values can be due to two causes: a different scattering mechanism (such as multiple scattering or shadowing) applies; or, the surface features responsible for producing the scattering are different for the two polarizations.

Figure 9 presents the first-order far field scattering results for an incidence angle of 60°, an rms height of λ, and various values of the surface slope. For H-polarization, the bistatic cross sections reflect the surface power-law decay in the back-propagation direction, but tend to flatten out in the forward direction. The peak in the forward direction is somewhat attenuated as the rms slope increases. For V-polarization, on the other hand, the peak in the forward direction is strongly attenuated as a function of surface slope. For both polarizations, the width of the peak decreases with increasing surface slope, reflecting the broadening of the peaks observed in Figure 6. The correlation between the two polarizations is high for the first order term, indicating that both H- and V-polarizations scatter from the same surface Bragg components. The relative phase difference between the two polarizations

is approximately 180°, consistent with a single bounce polarimetric signature.

Figure 10 presents the higher order field results for the same incidence angle. As expected from the source function results shown in Figure 6, the magnitude of the higher order scattered field is an order of magnitude smaller than the first order field, while the general shape of the bistatic cross section remains similar. The values for the HV correlation coefficient are low, indicating that the higher order fields scatter from different surface features for each incident polarization. This is in agreement with the calculated correlation between the source function for each polarization (result not shown). Finally, the HV phase difference, although noisy, is roughly zero. This is consistent with the interpretation of the higher order field as being due mainly to double scattering.

For higher incidence angles, the results for the first-order field are consistent with the previous discussion (see Figure 11 for the 89° incidence angle case). The main difference appears in the HV phase difference, whose mean is approximately 150°. This is consistent with the phase shift observed in the V-polarization source function in Figure 4. The results for the higher order field, on the other hand, are different in one significant respect: the HV phase difference is about 180°, consistent with an odd (rather than even) number of bounces. This behaviour is only observed for incidence angles $\theta_0 \geq 80°$, and increases with increasing slope. It suggests that, for very high incidence angles third order interactions, or higher, may dominate away from the specular direction.

7. Conclusions

I have presented a technique for separating first-order from higher order contributions to the surface current for scattering from perfectly conducting rough surface. Using this technique, I was able to examine the dependence of the single and multiple scattering components on incidence angle, rms surface height, rms surface slope and polarization. Given the results presented in this paper, one can make the following conclusions:

1. For higher incidence angles, there is a strong dependence of the first-order scattering coefficient on the surface slopes, especially for V-polarization.

2. For all the incidence angles studied, there was a discrepancy between the first-order coefficient and perturbation theory for the non-propagating modes for V-polarization.

3. Multiple scattering contributions increase with surface height, slope, and incidence angle.

4. Multiple scattering interactions are localized in momentum space.

5. Except for the highest incidence angles, higher order scattering is consistent with double-bounce scattering.

Appendix A

The periodic Green's function is given by [21]

$$g_p(\vec{r},\vec{r}') = \frac{i}{4}\sum_{m=-\infty}^{\infty} H_0^1\left(k\sqrt{(x-(x'+mL))^2+(z-z')^2}\right)\exp\left[imk\sin\theta_0 L\right] \qquad (16)$$

Veisoglu et al. [24] have evaluated the sum

$$S(a,b,r,s) \equiv \frac{i}{4}\sum_{m=-\infty}^{\infty} H_0^1\left(\sqrt{s^2(m+b)^2+a^2}\right)\exp\left[imr\right] \qquad (17)$$

$$= \frac{e^{ibs}}{\pi}e^{i(s+r)}\int_0^{\infty} du\, \frac{e^{-sbu^2}}{e^{su^2}-e^{-i(s+r)}}\,\frac{\cos\left(au\sqrt{u^2-2i}\right)}{\sqrt{u^2-2i}} \qquad (18)$$

where I use a slightly different notation from Veisoglu et al. to emphasize the symmetry properties of the sum

$$a = k(z-z') \qquad (19)$$

$$b = (x-x')/L \qquad (20)$$

$$s = kL \qquad (21)$$

$$r = kL\sin\theta_0 \qquad (22)$$

The integral is rapidly convergent and can be evaluated numerically. Given this sum, the periodic Green's function can be written as

$$g_p = \frac{i}{4}\left(\sqrt{(sb)^2+a^2}\right)\cdot S(a,b,r,s) + S(a,-b,r,s), \qquad (23)$$

While the previous expression provides an exact evaluation of the periodic Green's function, it is not convenient for use in Monte Carlo applications. The function $S(a,b,r,s)$ depends on the surface height through the parameter a. This means that S must be numerically integrated as many times as the number of elements in the MOM matrix. For large surfaces, this is impractical since it makes the matrix loading the most computationally expensive part, by far. To overcome this problem, I will make use of the fact that I am interested in surfaces which are much longer than the electromagnetic wavelength. From the definition of $S(a,b,r,s)$, one can show that the following identity holds:

$$\frac{i}{4}\sum_{m=1}^{N} H_0^1\left(\sqrt{s^2(m+b)^2+a^2}\right)e^{imr} = S(a,b,s,r) = e^{iNr}S(a,N+b,r,s) \qquad (24)$$

and the periodic Green's function can be written as

$$g_p = \frac{i}{4}\sum_{m=-N}^{N} H_0^1\left(\sqrt{s^2(m+b)^2+a^2}\right)e^{imr} = e^{iNr}S(a,N+b,r,s)+e^{-iNr}S(a,N-b,-r,s) \qquad (25)$$

Since $b \geq -1$, for long surfaces one will have that $s^2(2+b)^2 \gg a^2$, or, equivalently, that $1 >> (h-h')^2/L^2$, where h is the surface height. When this is the case, the exponential in the integrand of S will dominate the value of the integral and the parameter a will only have a small influence. This allows us to expand S in terms of a

$$S(a, N+b, s, r) \approx \sum_{n=0}^{n_{max}} a^n \frac{S^{(n)}(0, N+b, s, r)}{n!} \qquad (26)$$

where $S^{(n)}$ is the *nth* partial derivative of S with respect to a, and is easily obtained by differentiating equation (18). These integrals are also rapidly convergent and independent of the surface height so that they can be precomputed and stored in tables.

The numerical evaluation of the Green's function is performed by evaluating equation (25) and replacing S by its approximation equation (26). In this paper, I have chosen the surface length to be 102.4λ and the surface is sampled at 0.1A intervals. By comparing against the exact result, I have found that it is sufficient to take N = 1, and $n_{max} = 6$. All the integrals, as well as all subsequent calculations, were computed with double precision arithmetic. There is no absolute test of the numerical accuracy of the MOM results, but

there are some 1) CCWSM'% tests t owhichIsubjgtedt he 1 esult s. Mostimportantly,I checked t 11((degree of energy conservation: for all the results presented 11('1(. t he energy Conservation was better than ( ) . l°/0 , and in most cases it was better than 0.001 %. For selected surfaces, I also checked the periodicity of t he s ur.ace current, the reciprocity of the scatter-cd field, and the extinction of the field below t he sur f ace. All the results presented here satisfied these tests with good accuracy.

For t he vertical polarization calculations, it is necessary to compute the normal derivalive of the Green's function at t he sur face Using the previous r esults, one obtains t h e following expression

$$\hat{n} \cdot \nabla g_p = \frac{i}{4} \sum_{m=-N}^{N} H_1^1 \left(\sqrt{s^2 (m + b)^2 + a^2} \right) \frac{a + h_x s(m + b)}{\sqrt{s^2 (m + b)^2 + a^2}} + e^{iNr} Q(a, N + b, r, s, h_x) + e^{-iNr} Q(a, N - b, -r, s, h_x) \tag{27}$$

where h_x is the surface slope, and

$$Q(a, b, r, s, h_x) = k \frac{e^{ibs}}{\pi} e^{i(s+r)} \int_0^\infty du \frac{e^{-sbu^2}}{e^{su^2} - e^{-i(s+r)}} \left[\frac{h_x}{\sqrt{u^2}} (u^2 - i) \cos a u \sqrt{u^2 - 2i} + u \sin a u \sqrt{u^2 - 2i} \right] \tag{28}$$

This (expression is evalauted, in analogy with the expression for the periodic Green's function, by expanding Q in powers of a to six I.), or der.

Acknowledgements

The research described in this paper w as per formed t oy the Jet P1 opulsion Laboratory, California institute of Technology, under contract with the Office of Naval Research. I would like to thank Y. Kim and T.R. Michel for useful discussions related to the work reported here.

References

[1] S. Rice, "Reflection of electromagnetic waves from slightly rough surfaces," *Commun. Pure Appl. Math.*, vol. 4, pp. 351-378, 1951.

[2] M. Nieto-Vesperinas, "Depolarization of electromagnetic waves scattered from slightly rough random surfaces: a study by means of the extinction theorem," *J. Opt. Soc. Am.*, vol. 72, no. 5, pp. 539-547, 1982.

[3] M. Nieto-Vesperinas and N. Garcia, "A detailed study of the scattering of scalar waves from random rough surfaces," *Optica Acta*, vol. 28, no. 12, pp. 1651-1672, 1981.

[4] D. Winebrenner and A. Ishimaru, "Investigation of a surface field phase perturbation technique for scattering from rough surfaces," *Radio Science*, vol. 20, pp. 161-170, 1985.

[5] C. Eftimiu, "Modified wiener-hermite expansion in rough surface scattering," *J. Opt. Soc. Am.*, vol. 6, no. 10, pp. 1584-1591, 1989.

[6] E. Rodríguez and Y. Kim, "A unified perturbation expansion for rough surface scattering," *Radio Science*, vol. 27, pp. 799-931992.

[7] E. Thorsos and S. Broschat, "An investigation of the small slope approximation for scattering from rough surfaces. I. theory," *J. Acoust. Soc. Am.*, vol. 97, no. 4, pp. 2082-2093, 1995.

[8] A. Voronovich, "Small-slope approximation for electromagnetic-wave scattering at a rough interface of dielectric half-spaces," *Wave. Rand. Media*, vol. 4, no. 3, pp. 337-367, 1994.

[9] D. Holliday, 'Resolution of a controversy surrounding the kirchhoff approach and the small perturbation method in rough surface scattering theory," *IEEE Trans. Ant. and Prop.*, vol. 35, no. 1, pp. 120-122, 1987.

[10] A. Fung and G. Pan, "A scattering model for perfectly conducting random surfaces. i. model development," *Int. J. Remote Sensing*, vol. 8, no. 11, pp. 1579-1593, 1987.

[11] A. Ishimaru and J. Chen, "Scattering from very rough surfaces based on the modified 2nd-order kirchhoff approximation with angular and propagation shadowing," *J. Acoust. Soc. Am.*, vol. 88, no. 4, pp. 1877-1883, 1990.

[12] R. Axline and A. Fung, "Numerical computation of scattering from a perfectly conducting random surface," *IEEE Trans. Antennas Propag.*, vol. AP-26, pp. 482-488, 1978.

[13] E. 1. Thorsos, "The validity of the kirchhoff approximation for rough surface scattering using a gaussian roughness spectrum," *J Acoust. Soc. Am.*, vol. 83, pp. 78-92, 1988.

[14] E. 1. TI101SOS, "Acosutic scattering from a pierson-moskowitz sea surface," *J. Acoust. Sot. Am.*, vol. 1, pp. 335-349, 19!)(I.

[15] E. Rodríguez, Y. Kim, and S. Durden, "A numerical assessment of rough surface scattering theories: horizontal polarization" *Radio Science*, vol. 27, no. 4, pp. 497-513, 1992.

[16] Y. Kim, E. Rodríguez, and S. Durden, A numerical assessment of rough surface Scattering theories: vertical polarization," *Radio Science*, vol. 27, pp. 515-527, 1992.

[17] H. Ngo and C. Rino, "The application of beam simulation to scattering at low grazing angles part i: methodology and validation" *Radio Science*, vol. 29, no. 6, pp. 1365-1379, 1994.

[18] L. Tsang, C. Chan, K. Pak, 11. Sangani, and A. Ishimaru, "Monte Carlo simulations of large-scale composite random rough-surface scattering based on the banded-matrix iterative approach,)' *J. Opt. Soc. Am* vol. 1), no. 2, pp. 691-696. 1994.

[19] S. Lou, L. Tsang, C. Chan, and A Ishimaru, "Monte-Carlo simulations of scattering by a random rough surface with the finite-element method and the finite-difference method," *Microw. Opt.*, vol. 3, no. 5, pp. 150-154, 1990.

[20] P. Waterman, "Scattering by periodic surfaces," *J. Acoust. Soc. Am.*, vol. 57, no. 4, pp. 791-802, 1975.

[21] L. Tsang, J. Kong, and R. Shin, *Theory of Microwave Remote Sensing*. New York: Wiley-Interscience, 1985.

[22] G. Brown, "A stochastic fourier transform approach to scattering from perfectly conducting rough surfaces," *IEEE Trans. Ant. and Prop.*, vol. 30, no. 6, pp. 1135-1144, 1982.

[23] R. Harrington, *The Method of Moments*. MacMillan: New York, 1968.

[24] M. Veisoglu, H. Yueh, R. Shin, and J. Kong, "Polarimetric passive remote sensing of periodic surfaces," *J. Electro. Waves Applic.*, vol. 5, no. 3, pp. 267-280, 1991.

[25] T. Michel, M. Knotts, and K. O'Donell, 'Stokes matrix of a one-dimensional perfectly conducting rough surface," ,)(),$.4, vol 9, pp. 585-596, 1992.

Figure Captions

Figure 1: Figure 1a shows the percent of the surface illuminated as a function of the low-frequency cut-off. Figure 1b shows the rms slope (solid line) and rms curvature (dashed line) as a function of the low-frequency cut off The spectral decay power is -3 and tile rms height is $\sigma_h = \lambda$.

Figure 2: First-order perturbation coefficient for rms height $\sigma_h \lambda$, 45° incidence angle and A = 102.4λ (crosses), A = 51.2λ (diamonds), and A = 25.6λ (triangles). The magnitude of the coefficient as a function of wavenumber is shown in Figure 2a (V-polarization) and 2b (H-polarization). The phase of the first-order coefficient is shown in Figure 2c (V-polarization) and 2 d (H-polarization). The UPM first-order coefficient is shown as a solid line.

Figure 3: As in Figure 2, but for rms height $\sigma_h = 0.1\lambda$, 89° incidence angle.

Figure 4: As in Figure 3, but for rms height $\sigma_h = \lambda$.

Figure 5: V-polarization first order scattering coefficients for $\sigma_h = \lambda$, and incidence angles of 60° (a), 70° (a), 80° (a), and 85° (a). The surface conventions are as in Figure 2.

Figure 6: H-polarized (triangles) and V-polarized (crosses) first order (a,c) and higher order (b,d) source function magnitude for an incidence angle of 60° and an rms height of $\sigma_h = \lambda$. A = 102.4λ for Figures 6(a) and (b) A 25.6λ for Figures 6(c) and (d).

Figure **7:** As in Figure 6, but for an incidence angle of 89°.

Figure 8: H-polarization (triangles) and V-polarization (crosses) source function magnitude for an incidence angle of 89° and an rms height of $\sigma_h = \lambda$, for a surface whose **spectrum** has been **truncated at** λ. **A** = 102.4λ for Figures 8(a). A = 25.6λ for Figures 8(b).

Figure 9: Polarimetric parameters for the first-order source function for an incidence angle of 60° and an rms height of $\sigma_h = \lambda$. The surface conventions are as in Figure 2.

Figure 10: Polarimetric parameters for the higher-order source function for an incidence angle of 60° and an rms height of $\sigma_h = \lambda$. The surface conventions are as in Figure **2.**

Figure 11: Polarimetric parameters for the first-order source function for an incidence angle of 89° and an rms height of $\sigma_h = \lambda$. The surface conventions are as in Figure 2.

Figure 12: Polarimetric parameters for the higher-order source function for an incidence angle of 89° and an rms height of $\sigma_h = \lambda$. The surface conventions are as in Figure 2.

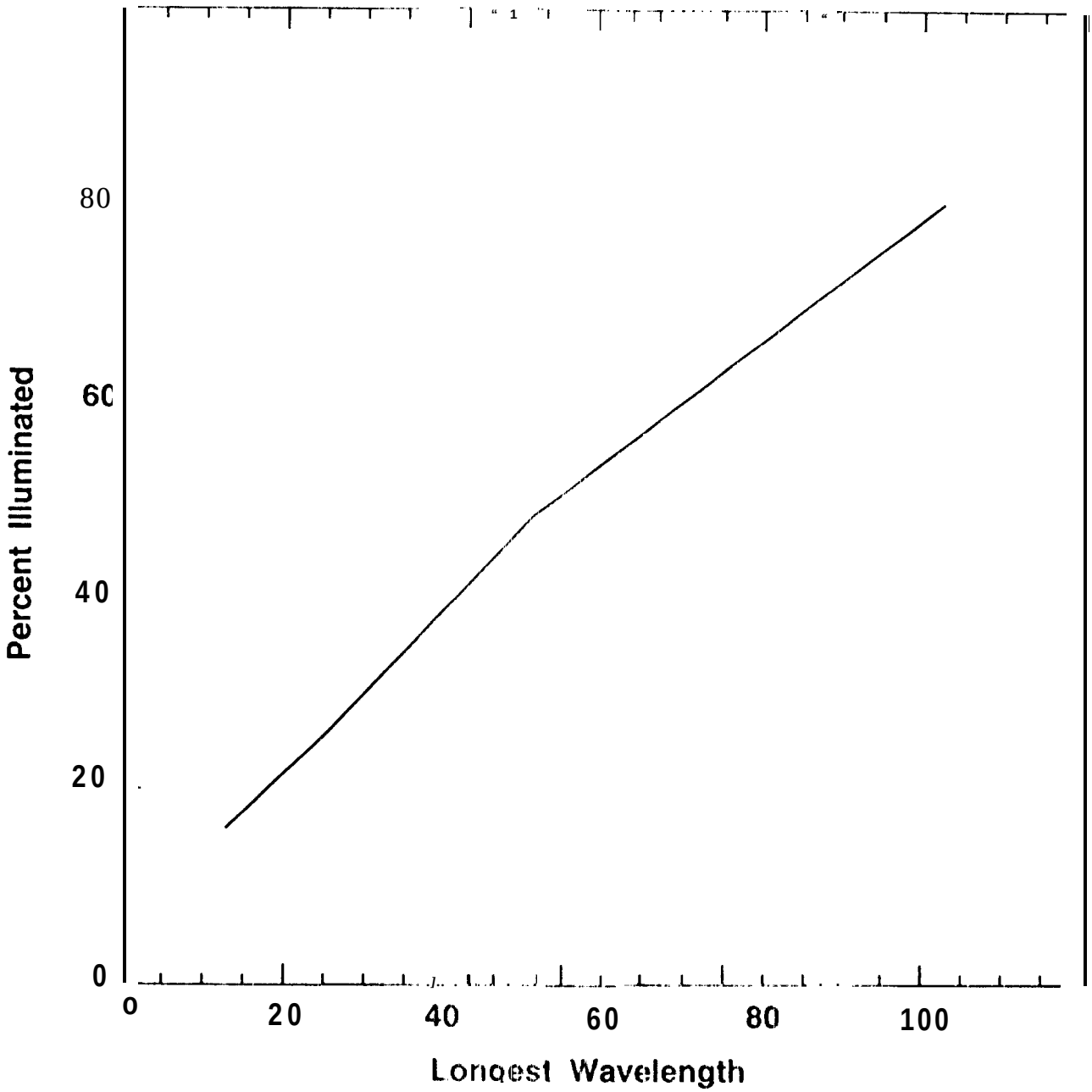
Percent Illuminated
80
60
40
20
0
0
20
40
60
80
100
Longest Wavelength

Figure 1a

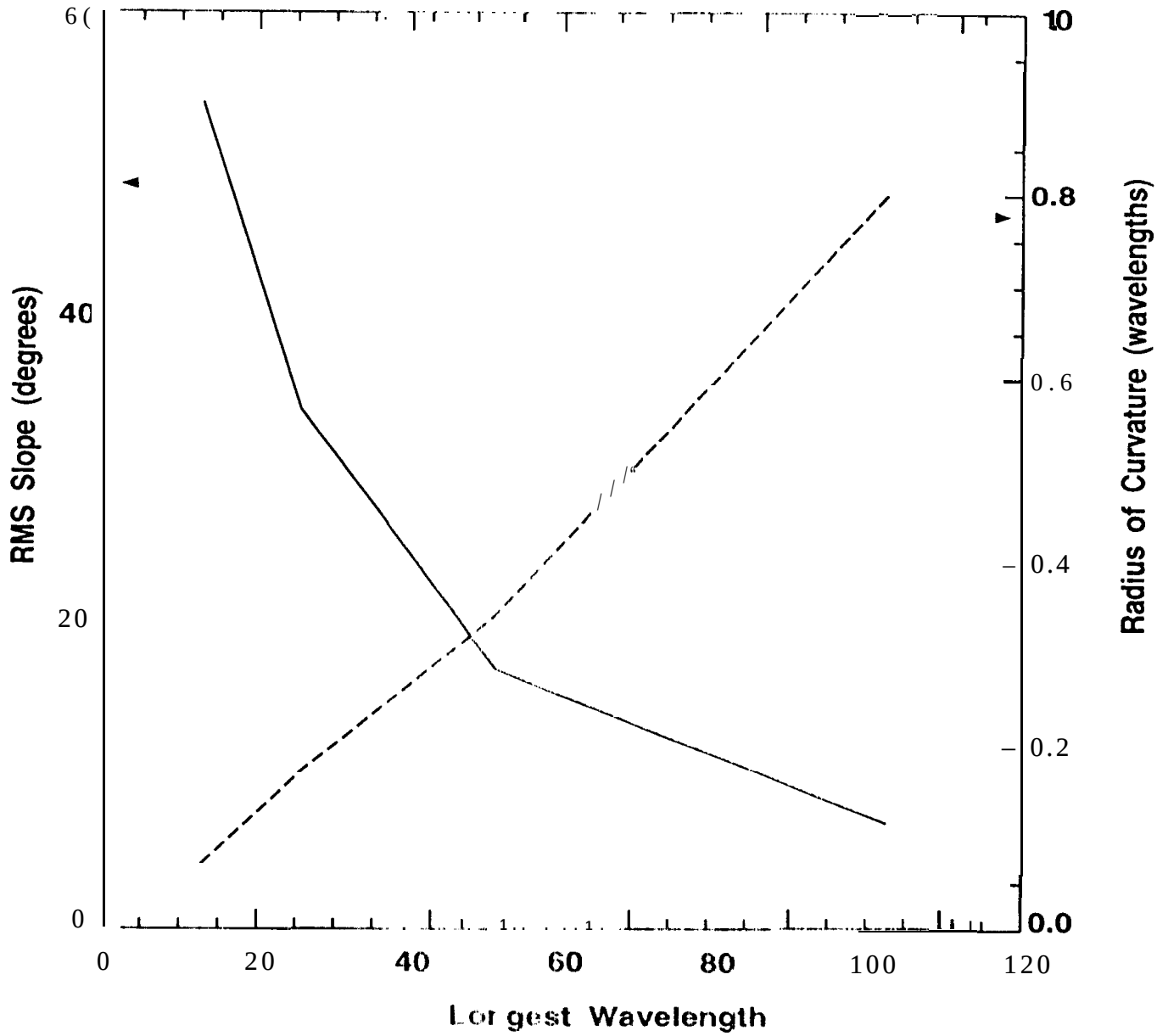
6(
40
20
0
RMS Slope (degrees)
10
0.8
0.6
0.4
0.2
0.0
Radius of Curvature (wavelengths)
0
20
40
60
80
100
120
Lor gest Wavelength

Figure 1b

(a)

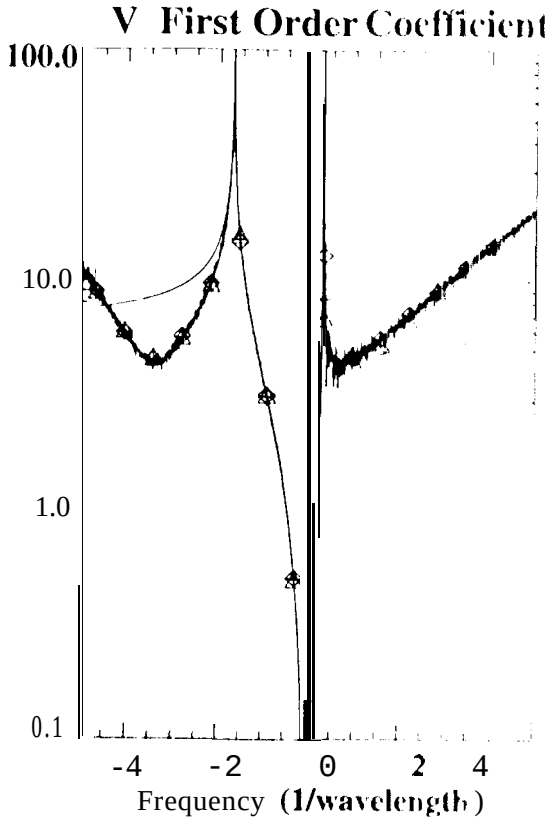

(b)

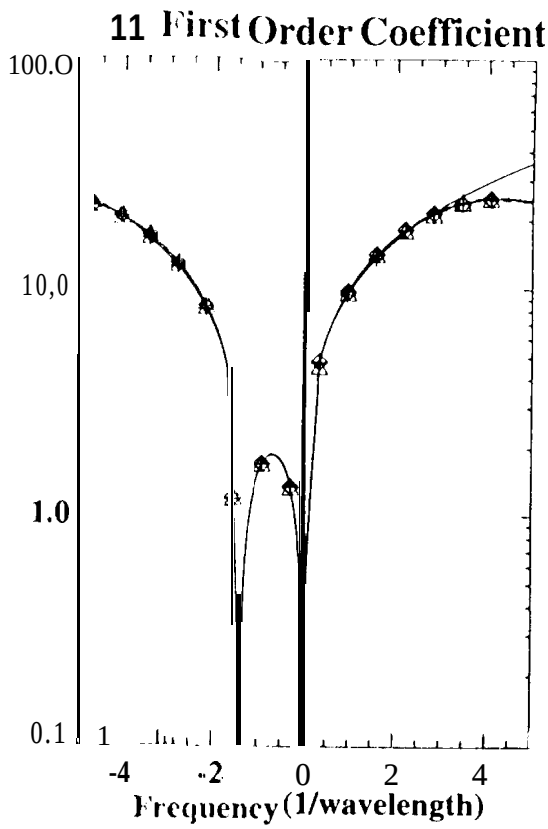

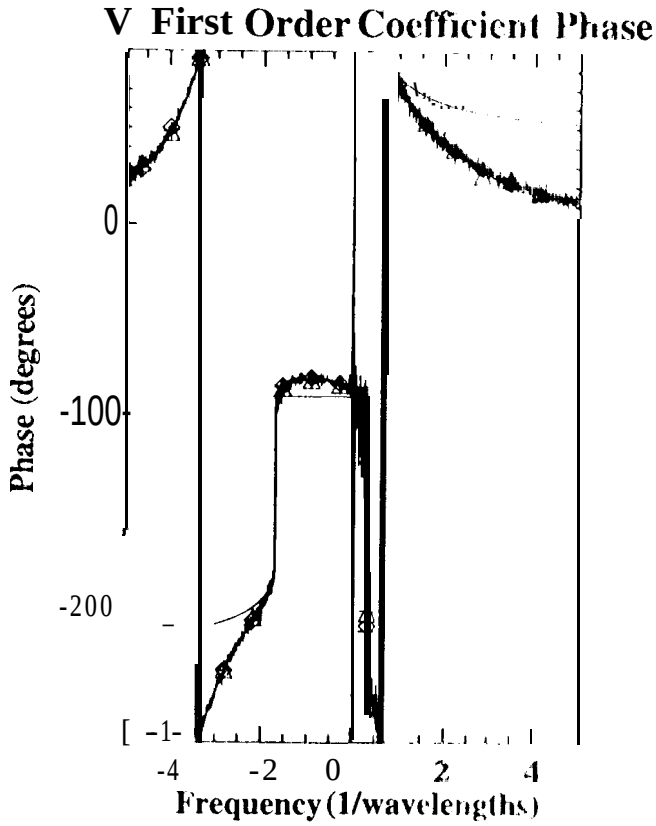

(c)

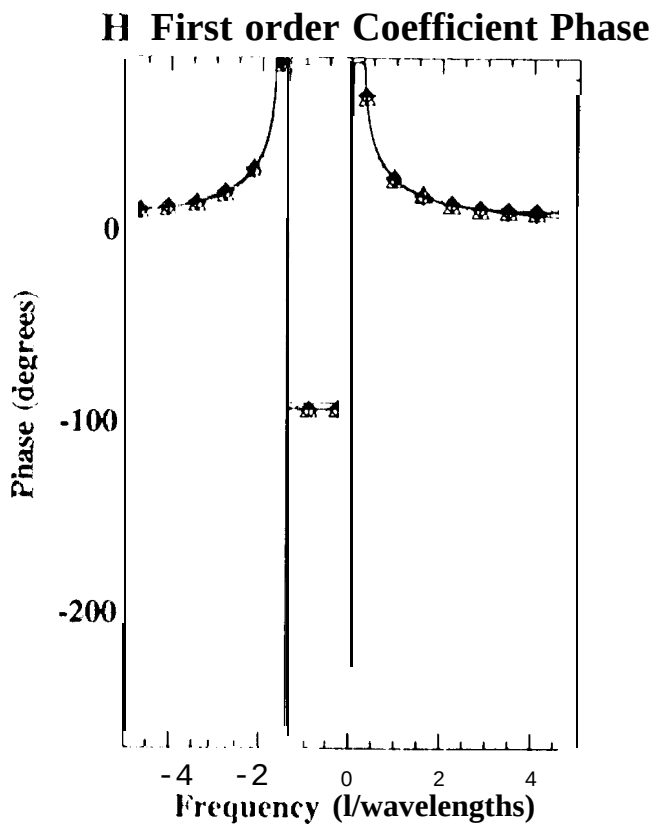

(d)

Figure 2

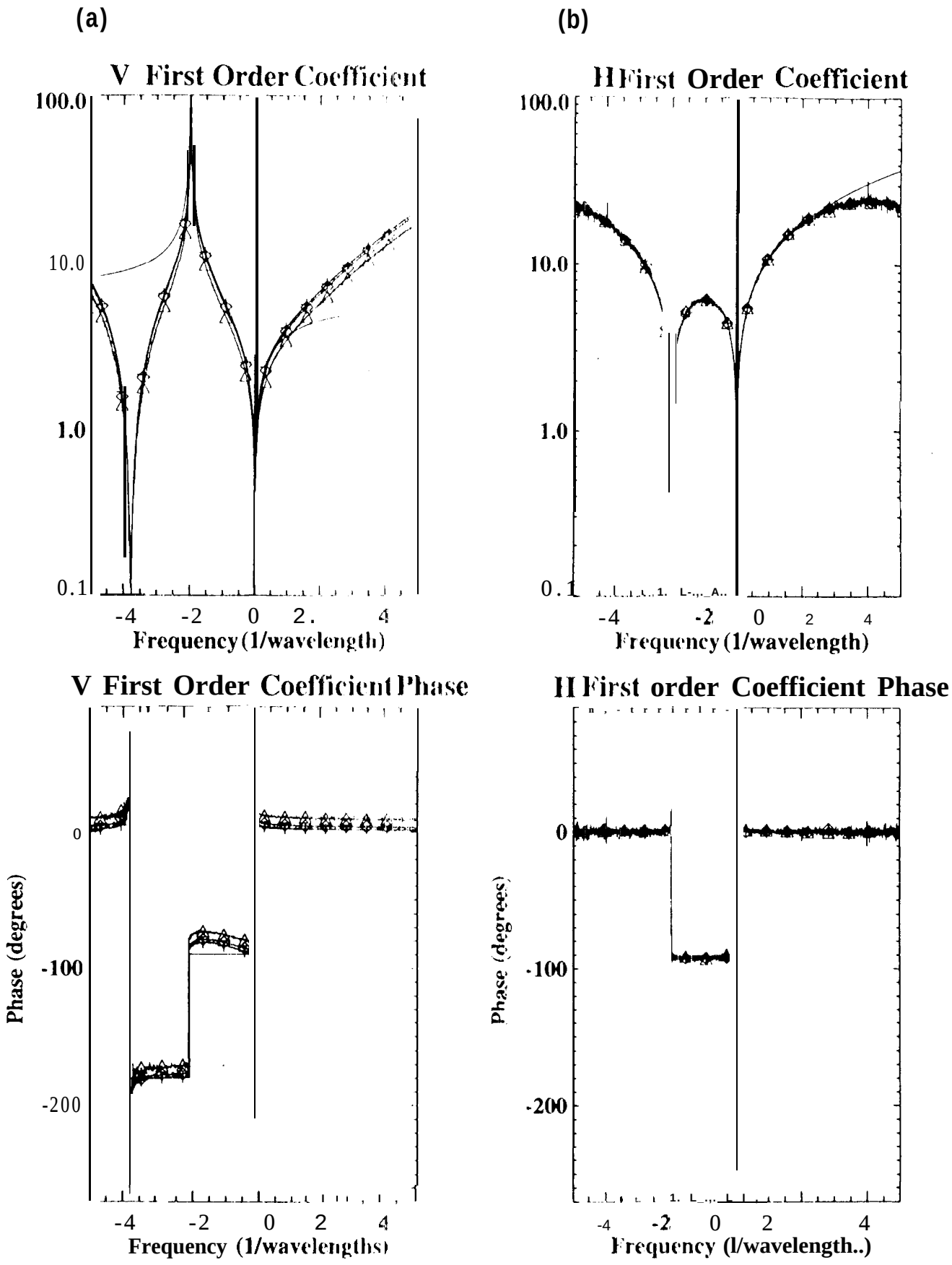
(a)
V First Order Coefficient
100.0
10.0
1.0
0.1
-4
-2
0
2
4
Frequency (1/wavelength)
(b)
H First Order Coefficient
100.0
10.0
1.0
0.1
-4
-2
0
2
4
Frequency (1/wavelength)
V First Order Coefficient Phase
Phase (degrees)
0
-100
-200
-4
-2
0
2
4
Frequency (1/wavelengths)
(c)
H First order Coefficient Phase
Phase (degrees)
0
-100
-200
-4
-2
0
2
4
Frequency (l/wavelength..)
(d)

Figure 3

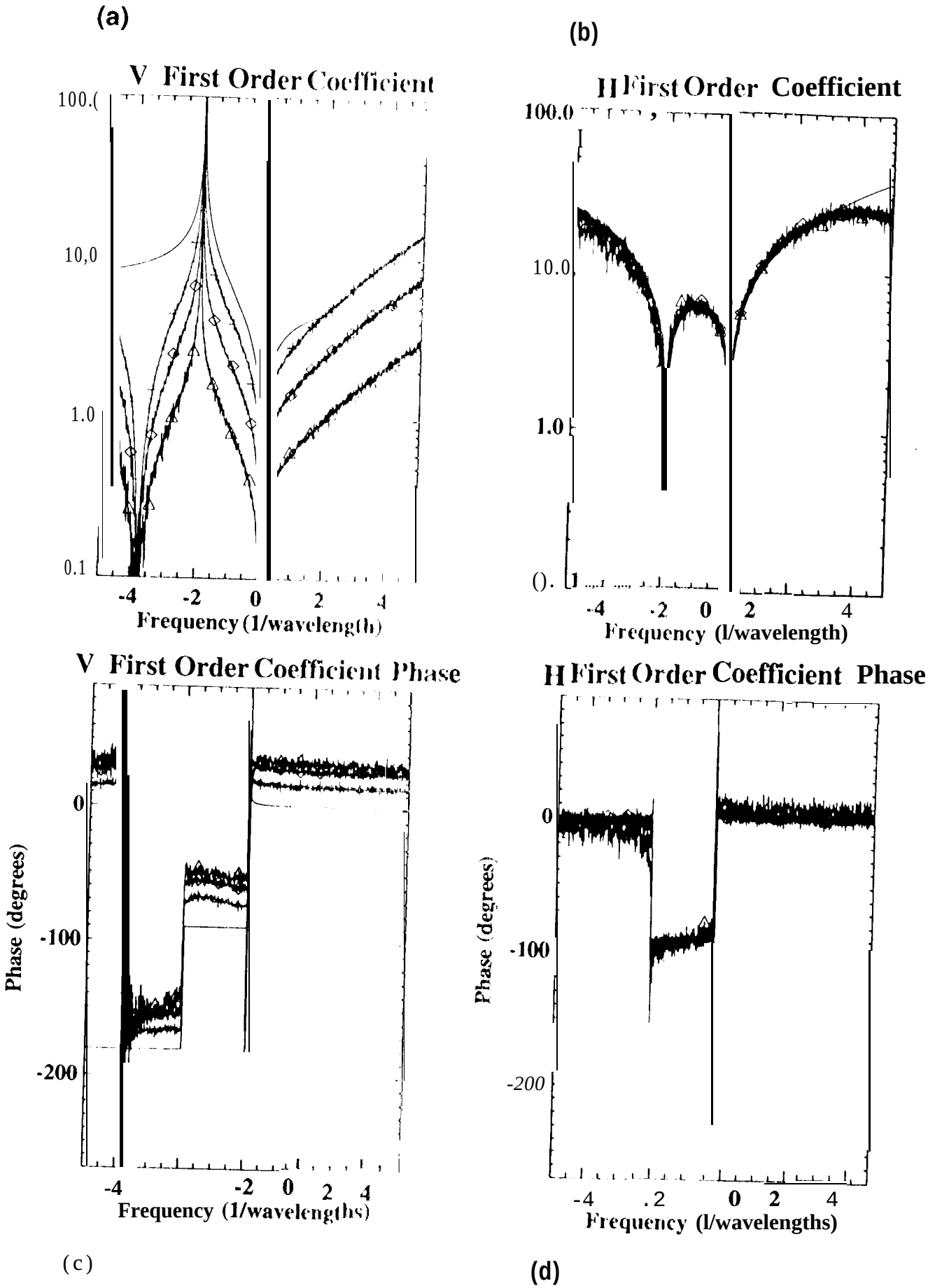
(a)
V First Order Coefficient
100.(
10,0
1.0
0.1
-4
-2
0
2
4
Frequency (1/wavelength)
(b)
H First Order Coefficient
100.0
10.0
1.0
().
-4
-2
0
2
4
Frequency (l/wavelength)
V First Order Coefficient Phase
0
-100
-200
Phase (degrees)
-4
-2
0
2
4
Frequency (1/wavelengths)
(c)
H First Order Coefficient Phase
0
-100
-200
Phase (degrees)
-4
.2
0
2
4
Frequency (l/wavelengths)
(d)

Figure 4

(a)

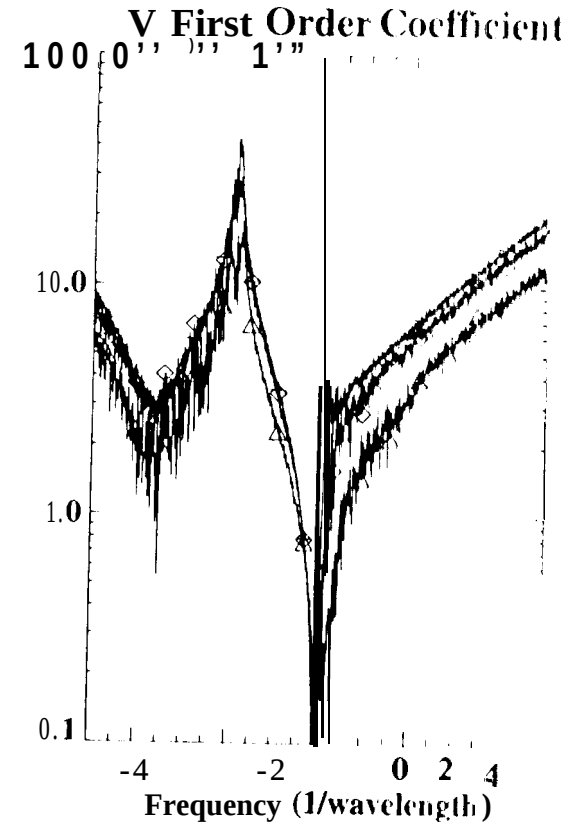

(b)

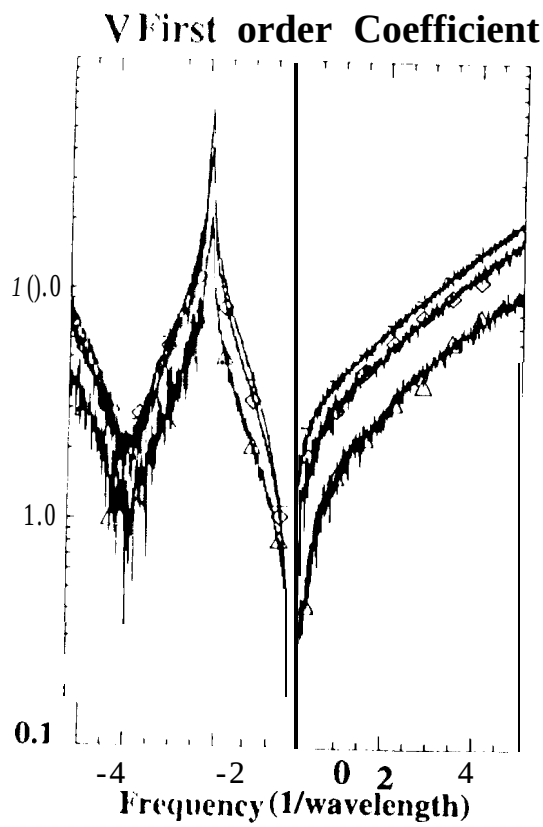

(c)

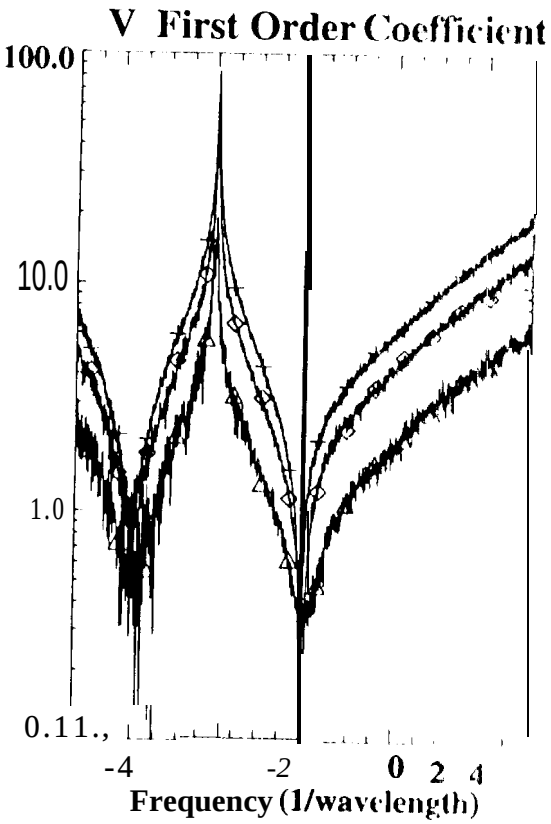

(d)

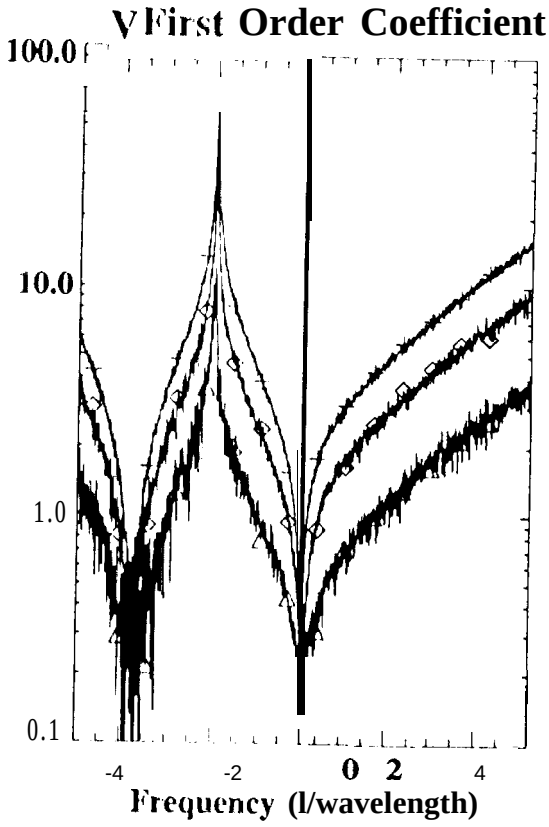

Figure 5

(a)

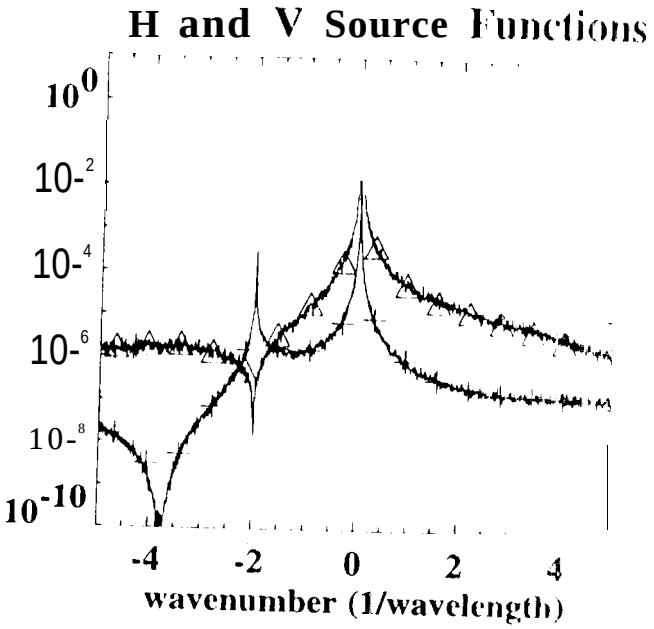

(b)

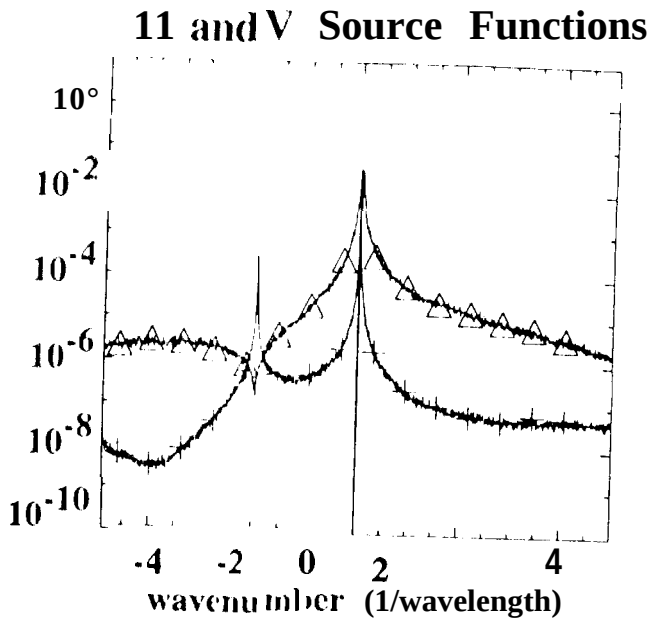

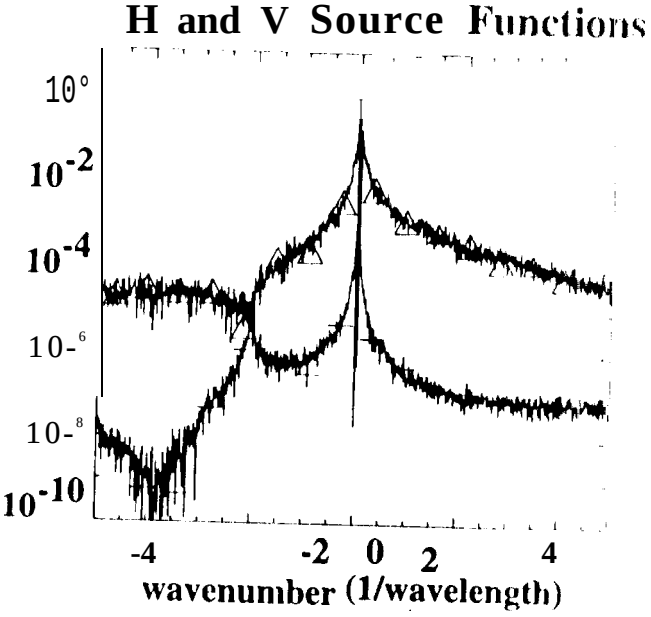

(c)

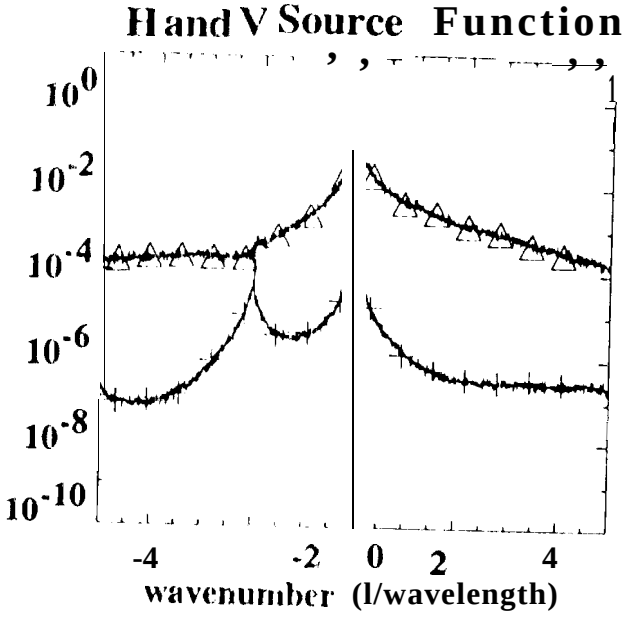

(d)

Figure 6

(a)

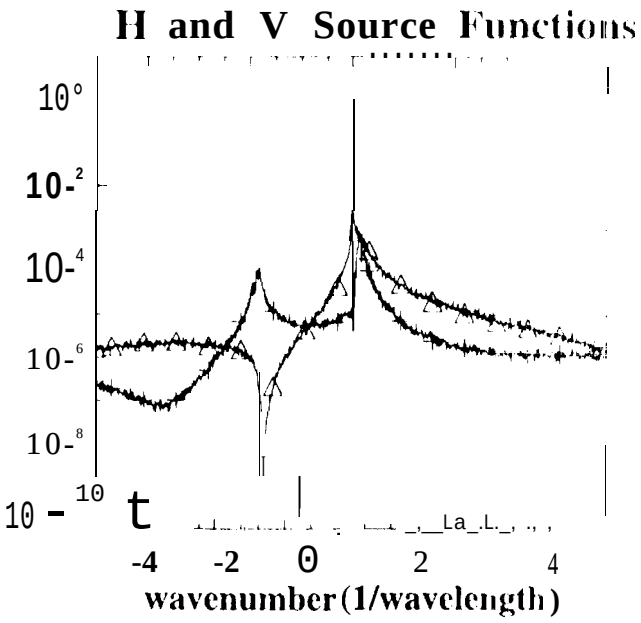

(b)

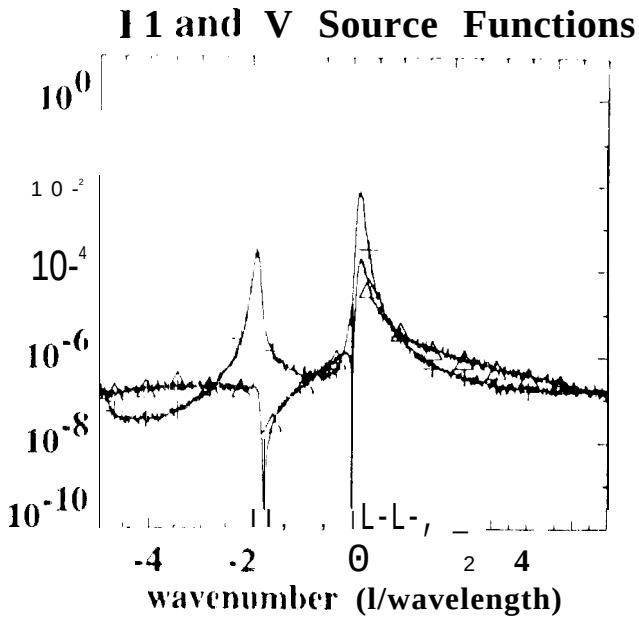

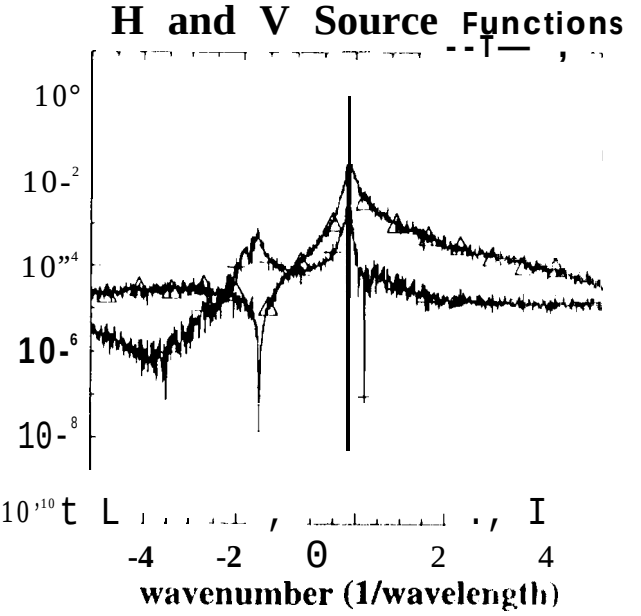

(c)

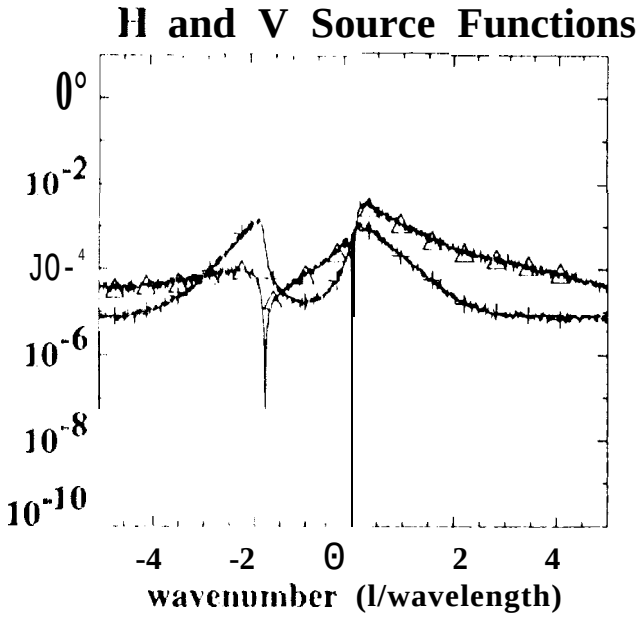

(d)

Figure 7

(a)

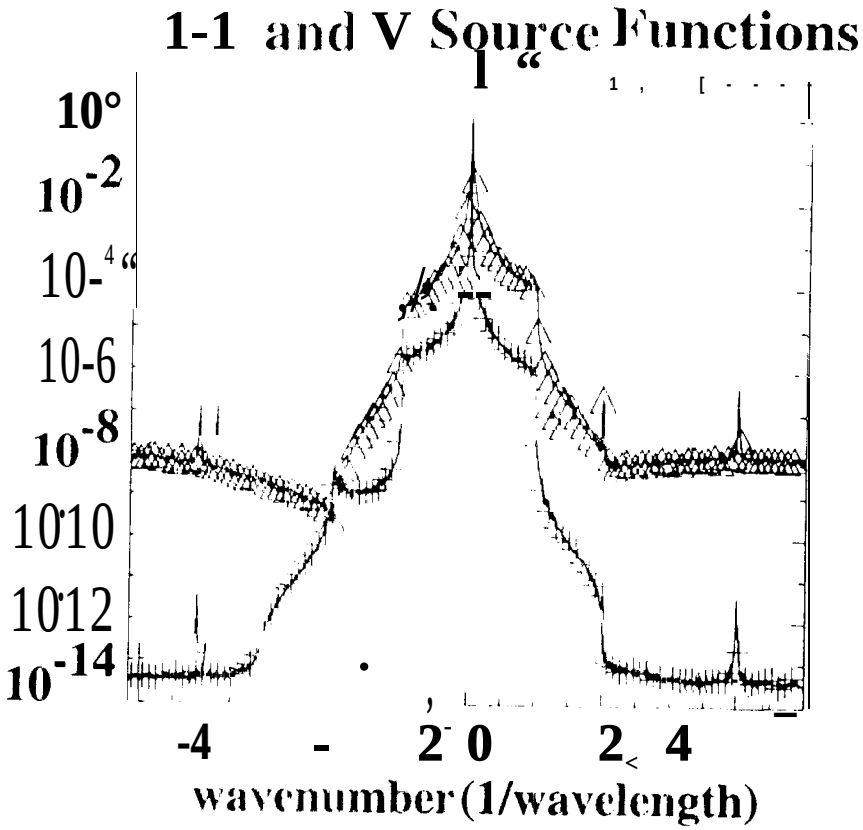
1-1 and V Source Functions
10°
10-2
10-4
10-6
10-8
1010
1012
10-14
-4
-2
0
2
4
wavenumber (1/wavelength)

(b)

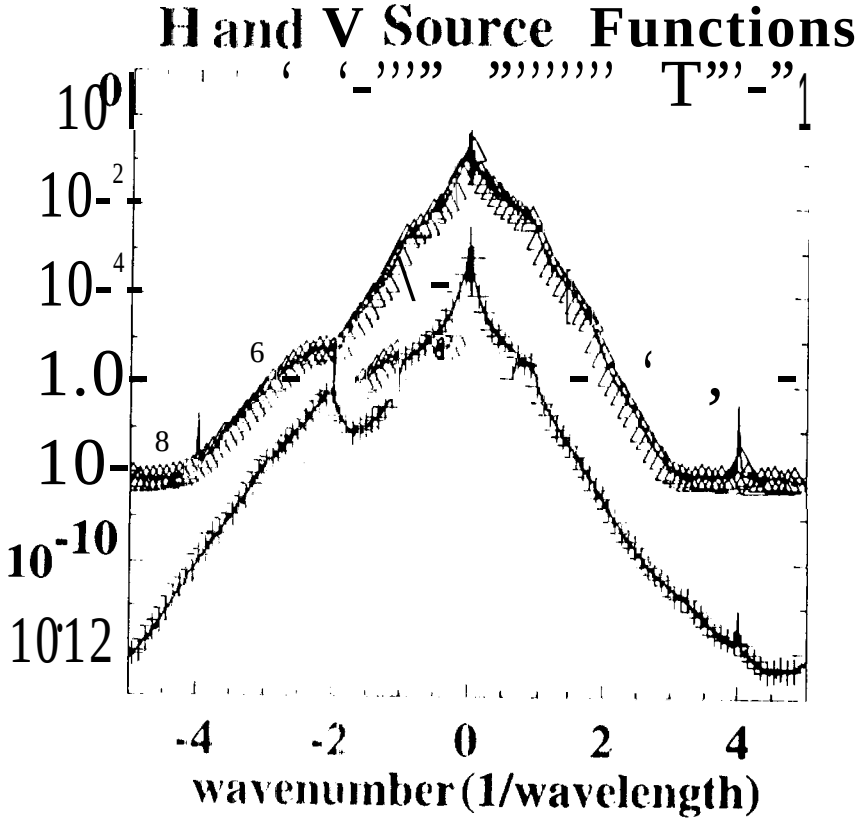
H and V Source Functions
10
10-2
10-4
1.0
10-10
1012
-4
-2
0
2
4
wavenumber (1/wavelength)

Figure 8

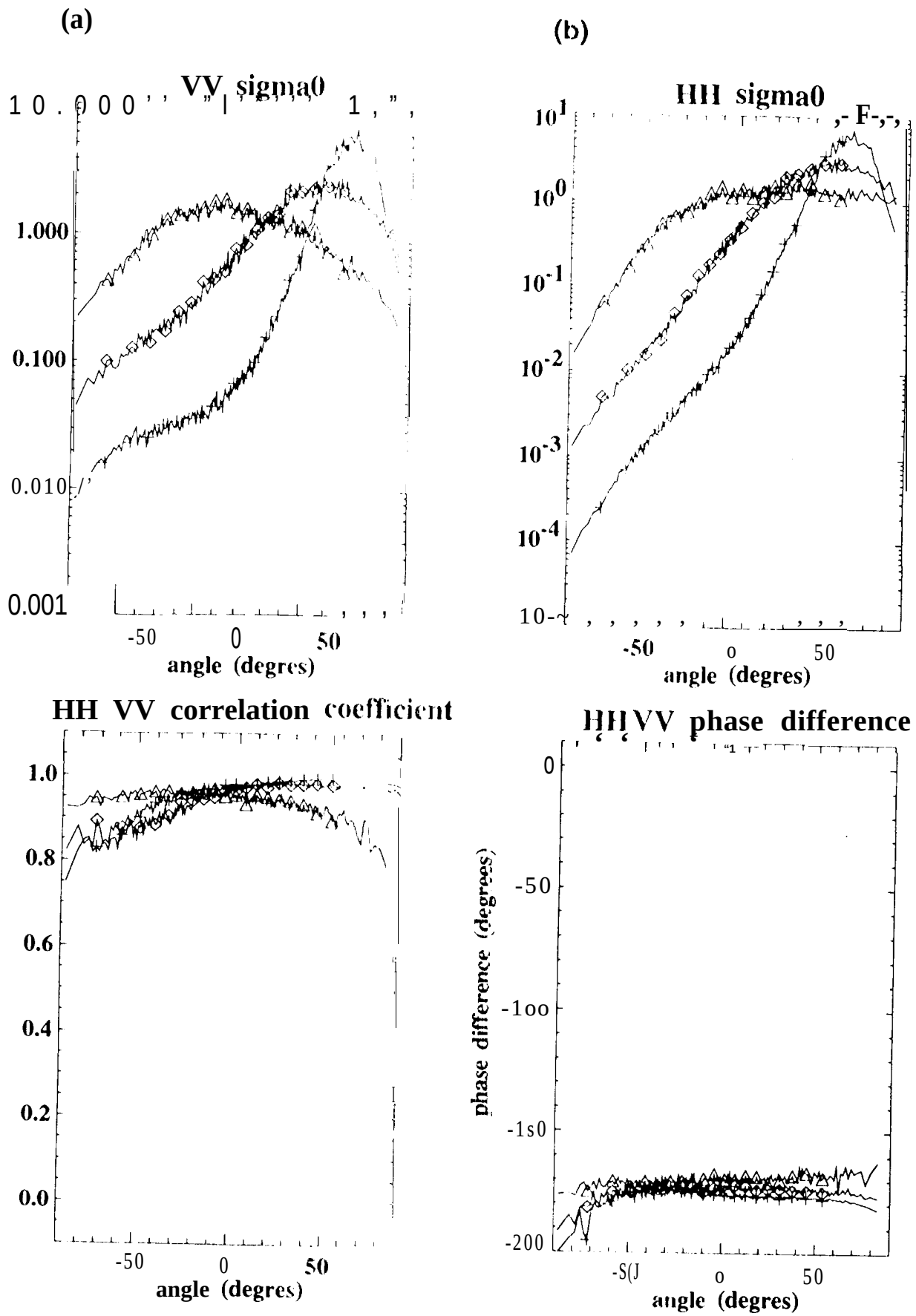
(a)
VV sigma0
1.000
0.100
0.010
0.001
-50
0
50
angle (degres)
(b)
HH sigma0
10^{1}
10^{0}
10^{-1}
10^{-2}
10^{-3}
10^{-4}
-50
0
50
angle (degres)
HH VV correlation coefficient
1.0
0.8
0.6
0.4
0.2
0.0
-50
0
50
angle (degres)
(c)
HH VV phase difference
phase difference (degrees)
0
-50
-100
-150
-200
-50
0
50
angle (degres)
(d)

Figure 9

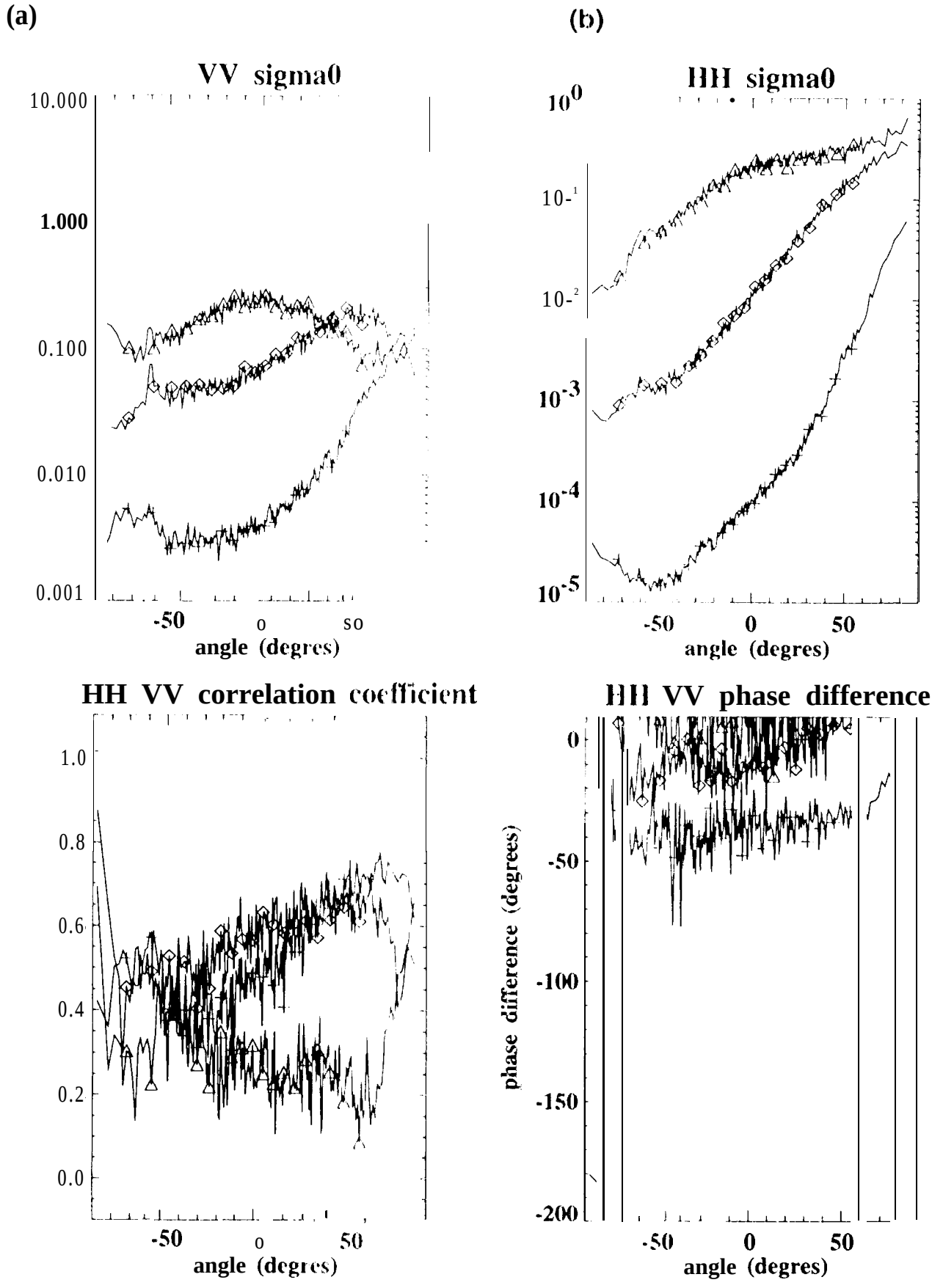
(a)
VV sigma0
10.000
1.000
0.100
0.010
0.001
-50
0
so
angle (degres)
(b)
HH sigma0
10^0
10^-1
10^-2
10^-3
10^-4
10^-5
-50
0
50
angle (degres)
HH VV correlation coefficient
1.0
0.8
0.6
0.4
0.2
0.0
-50
0
50
angle (degres)
HH VV phase difference
phase difference (degrees)
0
-50
-100
-150
-200
-50
0
50
angle (degres)
(c)
(d)

Figure 10

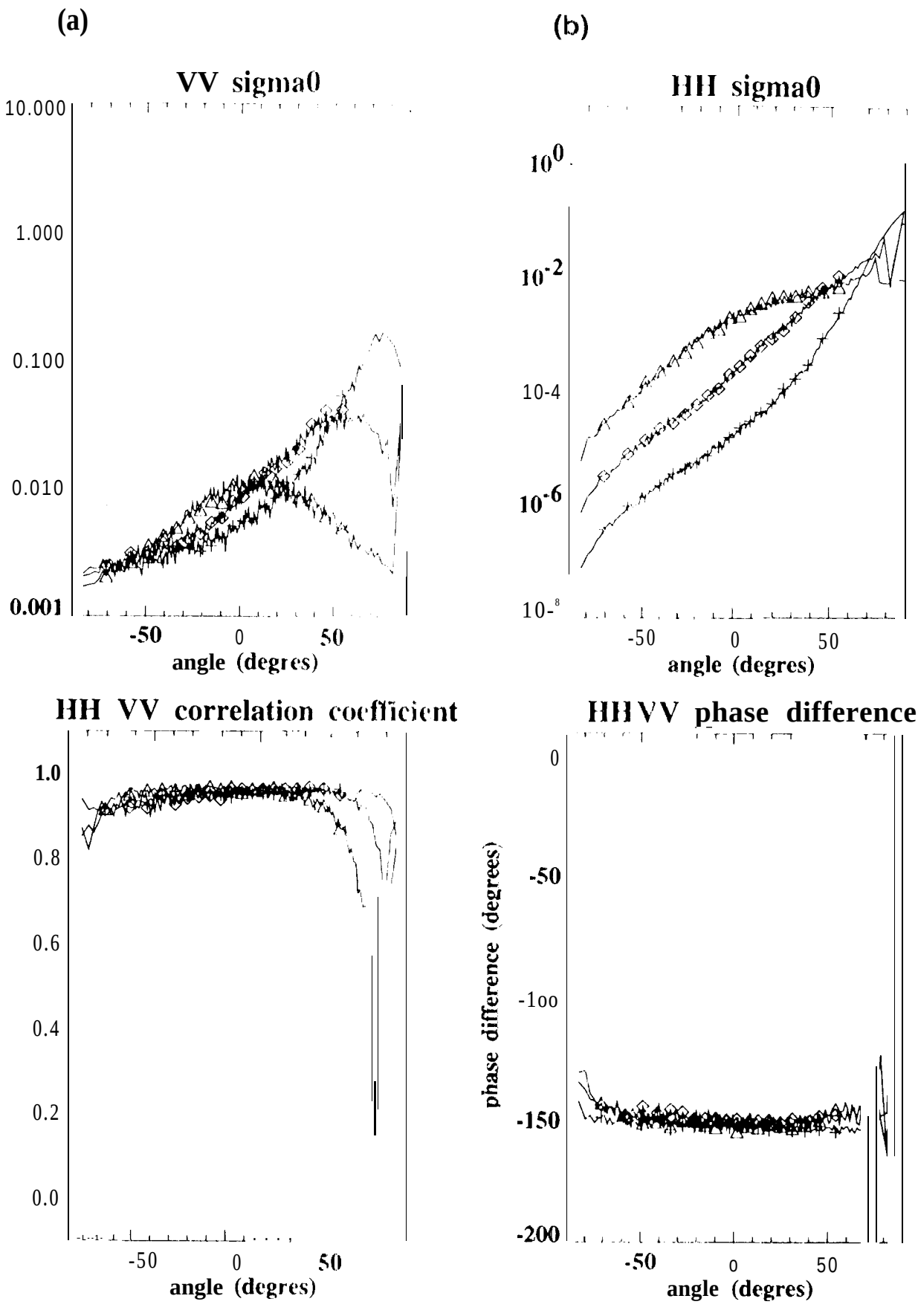
(a)
VV sigma0
10.000
1.000
0.100
0.010
0.001
-50
0
50
angle (degres)
(b)
HH sigma0
10^0
10^{-2}
10-4
10^{-6}
10^{-8}
-50
0
50
angle (degres)
HH VV correlation coefficient
1.0
0.8
0.6
0.4
0.2
0.0
-50
0
50
angle (degres)
(c)
HHVV phase difference
0
-50
-100
-150
-200
phase difference (degrees)
-50
0
50
angle (degres)
(d)

Figure 11

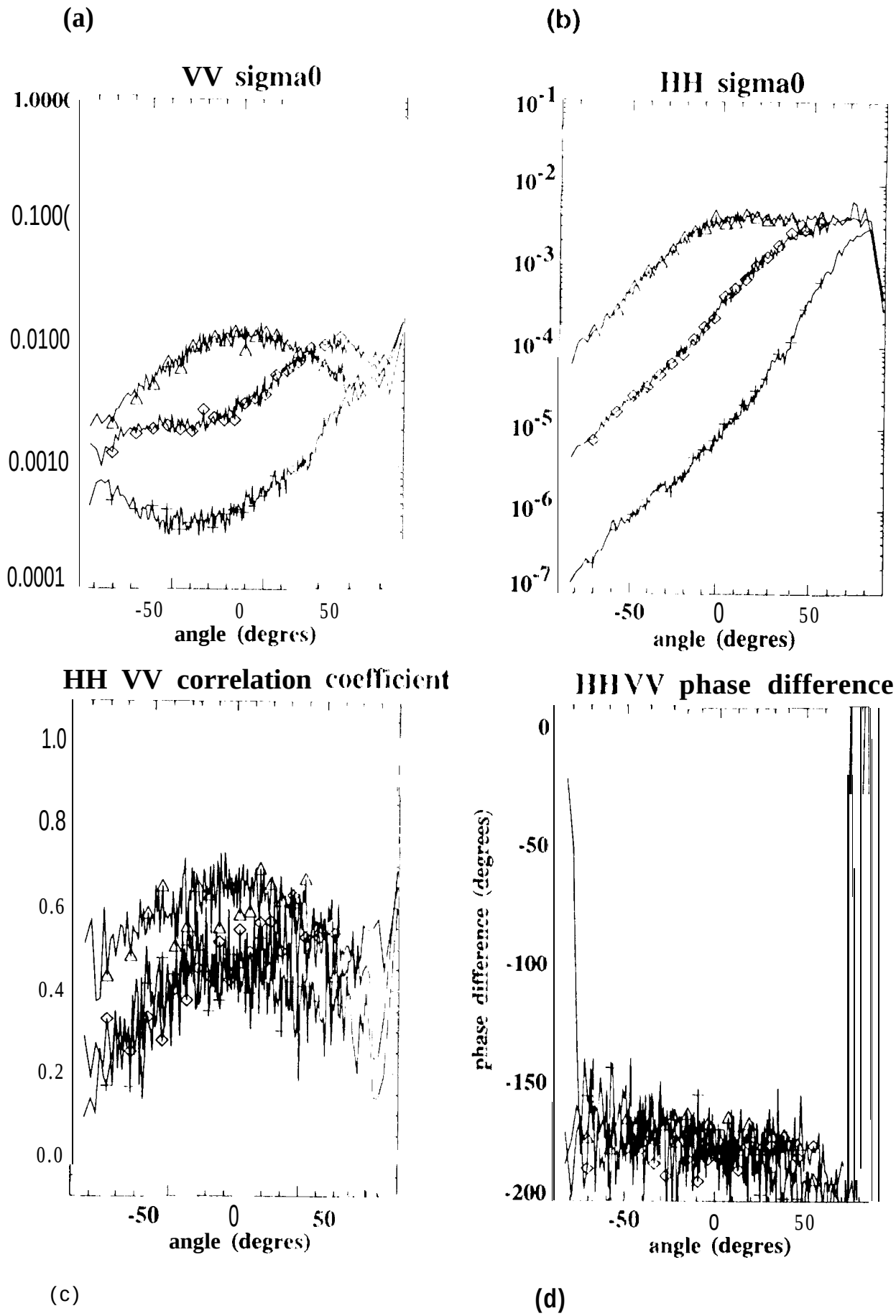
(a)
VV sigma0
1.0000
0.1000
0.0100
0.0010
0.0001
-50
0
50
angle (degrees)
(b)
HH sigma0
10-1
10-2
10-3
10-4
10-5
10-6
10-7
-50
0
50
angle (degrees)
HH VV correlation coefficient
1.0
0.8
0.6
0.4
0.2
0.0
-50
0
50
angle (degrees)
(c)
HH VV phase difference
phase difference (degrees)
0
-50
-100
-150
-200
-50
0
50
angle (degrees)
(d)

Figure 12